AIAA JOURNAL
Vol. 36, No. 12, December 1998

Thermal Model for Cracked Structures Repaired with Composite Patches

G. Renaud* and J. S. Hansen†
University of Toronto, Downsview, Ontario M4S 1C4, Canada

A finite element model is presented for examining the thermal history of adhesively bonded composite patches during and after cure. Transient heat conduction equations are solved to evaluate the temperature distribution in the system, especially during the postcure cooling process to obtain an accurate evaluation of the postcure thermal residual stresses. An example is presented showing the importance of the thermal evaluation, comparisons with previous studies are made to validate the model, and a simple thermal design study is presented. This model is intended for use in conjunction with a mechanical stress analysis model.

I. Introduction

COMPOSITE bonded patches, which now are considered as a mature technology, can be used to repair or reinforce aerospace structures by modifying their load distributions and bypassing defects or cracks. Temperature effects play a role in the mechanical behavior of this kind of repair in two ways: The temperature gradient distribution introduces thermal strains and stresses, and material properties are affected by the temperature distribution.

Two types of thermal stresses and strains can result from the curing procedure used during an adhesively patched repair. First, internal thermal stresses and strains that are a consequence of the patch curing procedure can manifest themselves in the composite patch. Second, residual stresses and strains can be present in the entire system because of the thermal mismatch between the various components when the system is allowed to cool to ambient temperature after the adhesive is cured.

Basically, two methods of applying a bonded composite repair to a structure can be used. The simpler technique is to cure the patch first and then bond it to the structure with a low-temperature curing adhesive. This ensures that little or no residual stress results from thermal interaction. However, the efficiency of the patch and the quality of the bond are higher when the patch is cured directly on the flawed area, using a high-temperature curing adhesive. Also, curing the patch on the structure makes possible the repair of curved surfaces of complex shape.

For the precure situation, only the composite patch is subjected to a temperature gradient. This gradient is the difference between the service temperature and the cure temperature and will result in the usual composite residual thermal strains and stresses. Thermal interaction is absent in the global model, and thermal analysis is therefore unnecessary.

Cocuring the patch involves heating the reinforced region at high temperature, under pressure, for a specific amount of time. If the reinforcing patch has a lower coefficient of thermal expansion than the plate being repaired, as is the case for carbon or boron fiber composite patches applied to the usual structural metals, tensile residual stresses develop in the plate on cooling after the cure. These stresses can jeopardize the integrity of the repair when they are added to the plate service loads. For example, a crack on the structure surface would tend to open even without the application of mechanical loads, causing a stress concentration at the crack tip.

Despite the importance of this problem, a very limited number of investigations can be found in the literature. Experimental studies[1,2] have been conducted to develop a simple formulation that can predict the peak magnitude of the stresses. However, analytical studies[3,4] have shown that this peak stress depends strongly on the mechanical boundary conditions of the problem. The results show that a clamped plate would be subjected to a much smaller state of thermal residual stresses than a plate that is allowed to expand freely.

To verify this behavior, a simple finite element analysis[4] has been made. The postcure cooling process has been modeled by forcing the temperature of the system to decrease from the cure to ambient temperature. The temperature was imposed through the entire model at each time step, and its rate of dissipation was constant. The value of the shear stiffness of the adhesive layer was regularly updated using a linear relationship with respect to the temperature, and the results agreed qualitatively with the analytical predictions.

Therefore, it is obvious that the thermal and the mechanical problems are interconnected. The thermal residual stresses depend in part on the mechanical boundary conditions, whereas the total stresses in the system subjected to mechanical loads depend on both mechanical loads and the thermal history.

In the model presented here the whole repair is considered as three distinct components: the host structure, which is seen as a plate that is damaged and in need of repair; the adhesive layer; and the patch. A typical single-sided repair configuration is illustrated in Fig. 1. Symmetric or nonsymmetric double-sided repairs also can be modeled by adding components or appropriate boundary conditions. A finite element mesh consisting of 8×8 elements to model the plate and 6×6 elements to model the patch is shown in Fig. 2 for the quarter-plate. The elements are made smaller in the vicinity of the crack tip to accurately capture the stress singularity. Similarly, the elements are made smaller in the y direction at the top edge of the patch to model the stress profile correctly in that area.

The mechanical aspect of this problem consists of evaluating the residual state of stress in the system as well as the stress intensity factor at the crack tip. However, the mechanical and fracture mechanics analyses are performed with an independent model that is unnecessary to present here.[5]

To get a good approximation of the thermal residual stress peak and profile, the actual temperature and temperature gradient distributions must be found with respect to both space and time. A realistic stress distribution of the whole system plate/adhesive/patch can be obtained using this approach. The flowchart of Fig. 3 illustrates this transient thermal analysis process when the heat source for the cure is removed.

II. Finite Element Formulation

The transient heat conduction equation, which represents the conservation of thermal energy, is the governing equation for the present heat transfer analysis. This equation can be written, without heat generation, as

$$\nabla \cdot ([\bar{k}]\{T\}) = \rho c \dot{T} \tag{1}$$

Received Nov. 4, 1997; revision received July 25, 1998; accepted for publication Aug. 19, 1998.

*Graduate Student, Institute for Aerospace Studies, 4925 Dufferin Street.
†Professor, Institute for Aerospace Studies, 4925 Dufferin Street. E-mail: hansen@bach.utias.utoronto.ca.

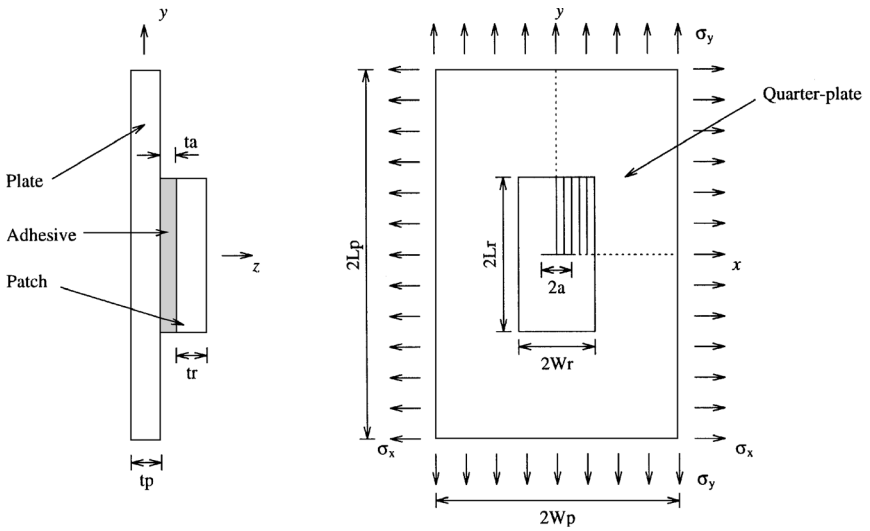

Fig. 1 Typical patch repair configuration.

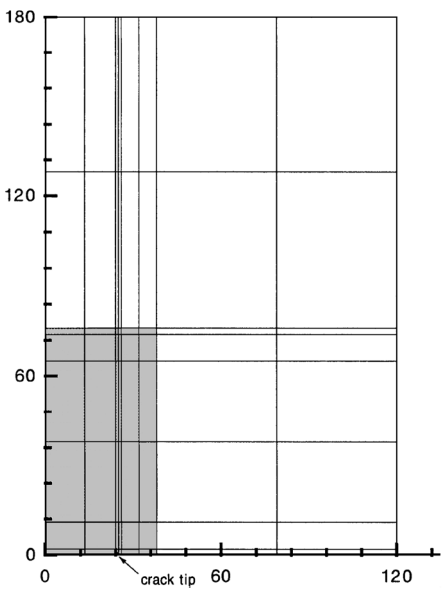

Fig. 2 Finite element discretization mesh.

where c is the material specific heat capacity, ρ is the density of the material, and $\dot{T}$ is the rate of change in the temperature. The term $[\bar{k}]$ is the thermal conductivity matrix for an anisotropic medium.

For this problem, the only boundary condition considered is the imposed temperature at some nodes. In addition to this boundary condition, initial conditions are specified for the transient thermal analysis.

After using the principle of virtual temperature and an implicit time integration method such as, in this case, the Euler backward difference method, the equation for virtual energy becomes

$$\int_V \mathrm{d}T^T \left(\frac{\rho c}{\Delta t}\right) T^{t+\Delta t}\,\mathrm{d}V - \int_V \mathrm{d}T^T \left(\frac{\rho c}{\Delta t}\right) T^t\,\mathrm{d}V + \int_V \mathrm{d}\{T'\}^T [\bar{k}]\{T'\}^{t+\Delta t}\,\mathrm{d}V = 0 \tag{2}$$

The element temperatures and temperature gradients are evaluated in Eq. (2) at time $t + \Delta t$; the same interpolation matrices are employed to calculate the element temperature at other times when incremental temperatures and incremental temperature gradients are present. Note that this equation assumes constant coefficients; that is, the properties ρ, c, and $[\bar{k}]$ are considered independent of temperature. Also, these properties are averaged over the thickness of the laminate using Ohm's law.

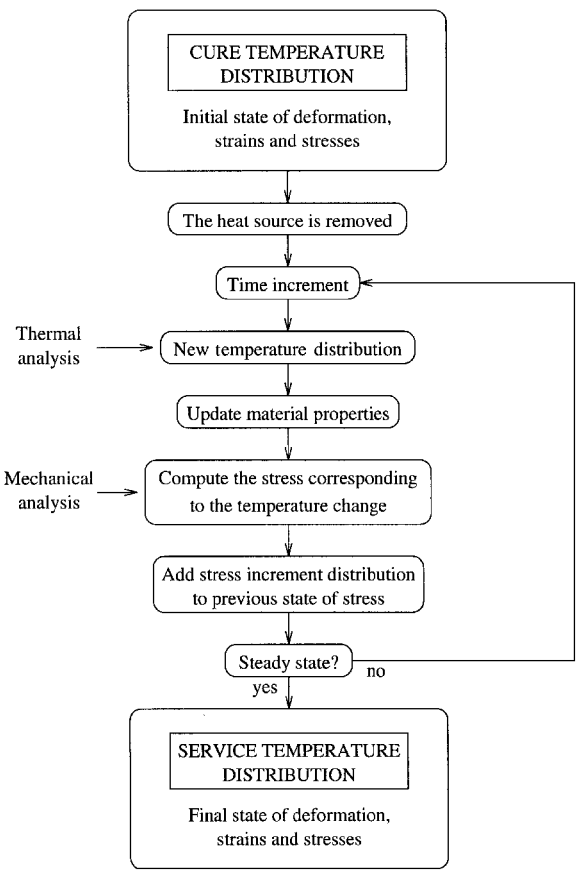

Fig. 3 Postcure cooling process flowchart.

A. Definition of Basis Function

The same mesh and elements are used in the mechanical and the thermal analyses. In the present case, the chosen basis functions are bicubic Lagrange polynomials for the patch and plate elements and bicubic–linear polynomials for the three-dimensional adhesive-layer elements. Also, with the present formulation the temperature variation is ignored through the thickness of the patch and plate elements. However, the temperature is allowed to vary linearly through the thickness of the adhesive-layer elements.

B. Simulation of Postcure Cooling Process

The simulation of the postcure cooling process is completed in a series of steps. These steps are related to Fig. 4, which represents

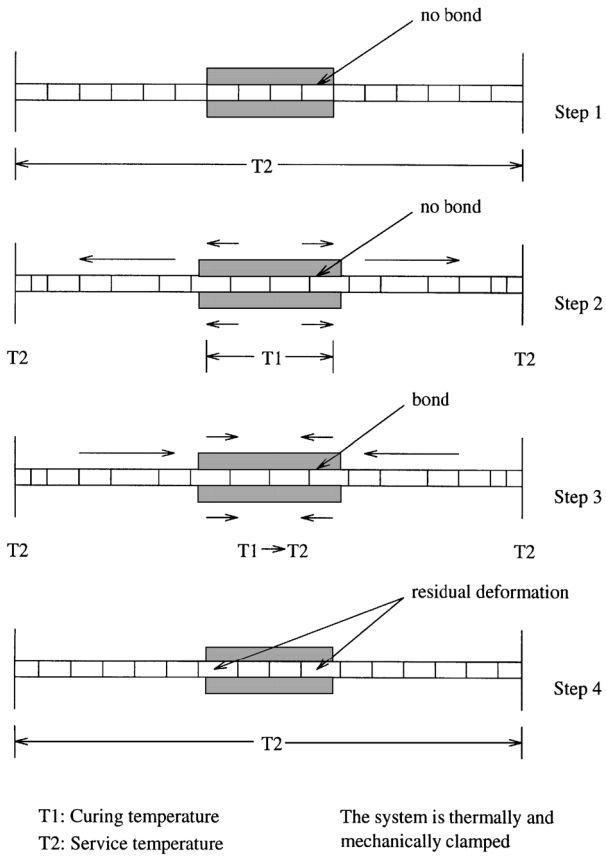

Fig. 4 Adhesive cure process.

the cure procedure. All of the finite element calculations, which are illustrated in the flowchart of Fig. 3, are completed in step 3.

1) The patch and the adhesive layer are placed on the plate, at ambient temperature. At this stage, no chemical reaction has taken place in the epoxy; therefore, there is no interaction between the different parts of the system.

2) The patch is heated until it reaches a specified temperature; the part of the plate removed from the patch zone is assumed to be at ambient temperature. This heating produces a steady temperature distribution in the system; hence, thermal deformation is induced in the plate, the adhesive layer, and the patch. The amount of the individual deformation, however, is different because of the different coefficients of thermal expansion. Furthermore, the patch is free to expand but the plate can be clamped or have any displacement restriction. At this point, the patch and the adhesive layer are still free of stress and there is still no interaction between the parts of the system. Because of the boundary condition and the heating of a segment of the plate, thermally induced stresses and strains are present in the plate. This state is maintained for a specific amount of time.

3) When the cure is completed, the system is allowed to cool to ambient temperature. The temperature and the temperature gradient distributions change progressively until they reach a new steady state at ambient temperature. The way and the rate at which the heat is dissipated depend on the properties of the materials and on the thermal boundary conditions. Again, different parts of the system will deform, trying to recover their initial configuration at ambient temperature, a condition that is impossible because they are now linked. This cooling process is analyzed using a time-marching analysis in which the material properties are updated regularly as functions of temperature. During the process, the mechanical properties, which depend on temperature, are different for each node and at each time step. The incremental state of stresses in the system is computed and added at each time step. Although they lie on linear thermal and structural equations, the results from this analysis are dependent on the thermal history. The cooldown process is therefore nonlinear.

4) At ambient temperature, a state of residual thermal stress is present in the plate. Bending also can be induced if the repair is not symmetric. This initial state is then the starting point for any analysis involving the application of mechanical or thermal loads.

III. Numerical Example

A rectangular aluminum plate possesses a centrally located horizontal through-thickness crack. To prevent the propagation of the crack, a nontapered unidirectional boron–epoxy patch is considered. A patch would be applied on each side of the plate with its fibers oriented perpendicular to the crack. The plate and the adhesive layer have thicknesses of 4.48 and 0.1016 mm, respectively, and each patch is composed of six plies with a thickness of 0.127 mm each. The other dimensions and the material properties are given in Fig. 1 and Table 1, respectively.

It is assumed that the plate supports an in-service uniform tensile stress σ_0 of 300 MPa in the y direction, and it is assumed for simplification that the service temperature is 0°C.

Because the problem is symmetric with respect to the x axis, the y axis, and the midplane of the plate, it is possible to model the top half of the quarter-plate only. The finite element mesh used to model this problem is presented in Fig. 2.

Boundary conditions are imposed to ensure symmetry. They are u and $\phi_x = 0$ on the vertical axis of symmetry and v and $\phi_y = 0$ on the horizontal axis of symmetry. However, no v restriction is imposed on the nodes that are on the edges of the crack in order to permit crack opening. Also, all transverse degrees of freedom ϕ_x, ϕ_y, and w of the plate are constrained to force symmetry with respect to the midplane. This restriction does not apply to the patch, which can bend.

The unpatched situation is considered first. This analysis is made to evaluate the stress state of the plate under service loads in the absence of the patch.

The σ_y stress field is illustrated in Fig. 5, where the direction perpendicular to the mesh corresponds to the magnitude of the stress and the shaded area corresponds to the reference plane $\sigma_y = 0$.

It can be seen that most of the plate is under a constant stress, which is equal to the applied stress σ_0. However, in the vicinity of the crack tip, the stress increases abruptly. The shape of this singularity corresponds to the stress intensity factor for the mode I opening, which is 2746 MPa · mm$^{1/2}$. Furthermore, it can be seen that the stress on the edge of the crack is zero, as it should be because it is a free edge. The zero stress condition on the free edge is not imposed in the analysis but illustrates the accuracy of the finite element model.

Table 1 Material properties of components of patched aluminum plate

Component	Property
Aluminum plate	$E_p = 70.0\text{E}3$ MPa
	$k_p = 204$ mW/mm · °C
	$\nu_p = 0.3$
	$\rho_p = 2.707\text{E}{-6}$ kg/mm^3
	$\alpha_p = 23.0\text{E}{-6}$ °C^{-1}
	$c_p = 896.0\text{E}3$ mJ/kg · °C
Boron–epoxy patch	$E_{1r} = 208.1\text{E}3$ MPa
	$G_{23r} = 4.94\text{E}3$ MPa
	$\alpha_{2r} = 23.1\text{E}{-6}$ °C^{-1}
	$\rho_r = 2.0\text{E}{-6}$ kg/mm^3
	$E_{2r} = 25.44\text{E}3$ MPa
	$\nu_{12r} = 0.1677$
	$k_{1r} = 50$ mW/mm · °C
	$c_r = 840.0\text{E}3$ mJ/kg · °C
	$G_{12r} = G_{13r} = 7.24\text{E}3$ MPa
	$\alpha_{1r} = 0.17\text{E}{-6}$ °C^{-1}
	$k_{2r} = 1$ mW/mm · °C
Adhesive layer	$G_a(0°\text{C}) = 965$ MPa
	$\alpha_a = 23.1\text{E}{-6}$ °C^{-1}
	$c_a = 840.0\text{E}3$ mJ/kg · °C
	$G_a(100°\text{C}) = 0$ MPa
	$k_a = 0.75$ mW/mm · °C
	$\nu_a = 0.3$
	$\rho_a = 2.0\text{E}{-6}$ kg/mm^3

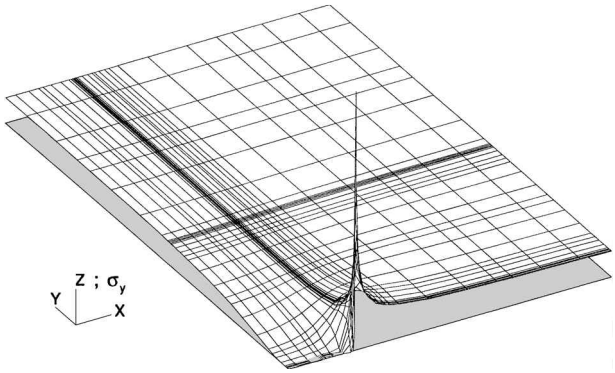

Fig. 5 The σ_y stress field for the unpatched situation (mesh of the Gauss points).

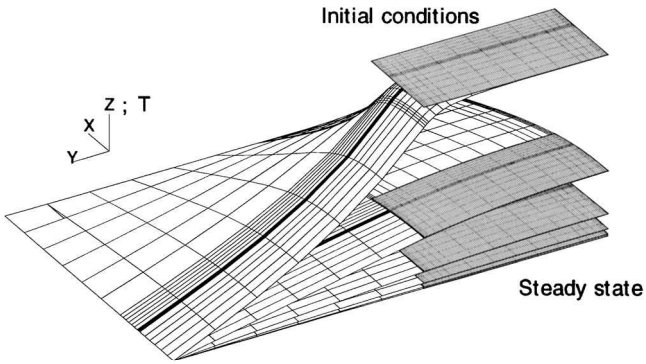

Fig. 6 Nodal temperature distributions during the cooling process (mesh of the Gauss points).

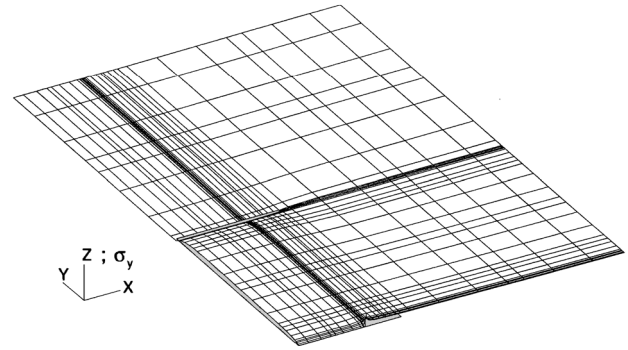

Fig. 7 Postcure thermal residual σ_y stress field in the patched plate (mesh of the Gauss points).

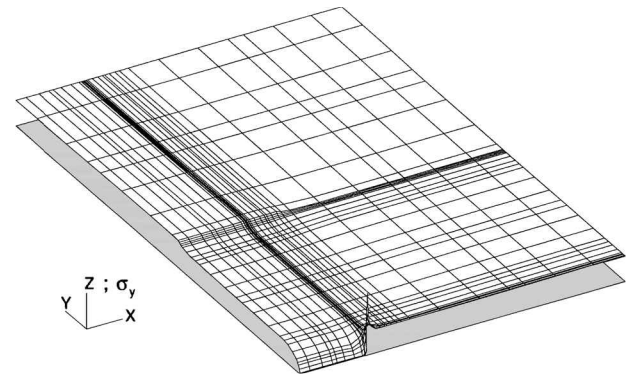

Fig. 8 Total σ_y stress field in the patched plate (mesh of the Gauss points).

If it is assumed that the patch can be bonded to the plate in the absence of the structural loads, the thermal analysis capabilities of the code can be used to obtain a postcure state of the residual thermal stresses.

The initial state of the postcure cooling-process modeling must ensure that the adhesive is at least at its cure temperature. This initial state can be seen as the first step when modeling the bonding of a precured patch or as the step following the cure of the composite patch in a cocured situation. It also is assumed that the temperature has been maintained for enough time to ensure that the polymer chemical reactions are completed by the time the system starts to cool.

In the present case, the patch is heated to 150°C but the plate edges are maintained at ambient temperature. This initial state and the subsequent cooling state are illustrated in Fig. 6.

It can be seen that the temperature is high and uniform over the patch in the initial state, as it was imposed by the thermal initial conditions, whereas it is distributed in the plate from ambient temperature at the edges to a maximum under the patch. It can be seen that the heating temperature of 150°C on the patch was enough to ensure that all of the plate nodes under the patch are above 100°C during the heating phase; hence the whole adhesive-layer temperature is above the cure temperature. The high temperature needed is due, in this case, to the near boundaries of the plate, which act as a heat sink.

At each time step, the adhesive-layer material properties were updated and an incremental state of stress was added until the total state of residual thermal stresses was reached at ambient temperature. The present case used five steps of 100 s to reach the convergence criteria that the temperature at every node must be less than 1°C above ambient temperature. The resulting σ_y distributions in the plate are presented in Fig. 7.

A tensile σ_y stress field is present in the patched area of the plate and the slight opening of the crack resulted in a thermal stress intensity factor K_I of 125 MPa · $mm^{1/2}$. On the other hand, a compressive σ_y field is present in the patch.

The service loads are added to the system once the postcure state of thermal residual stresses is known. The resulting state of σ_y stresses in the plate is illustrated in Fig. 8.

The plate σ_y stress is similar to the unpatched situation in that the plate is uniformly stressed by σ_0 on almost all of its surface. However, the stress is significantly lower under the patch because there is a load transfer through the adhesive layer in the composite laminate. Also, it is obvious from the shape of the singularity at the crack tip that the stress intensity factor K_I is much smaller than in the unpatched situation. Indeed, its value is 624 MPa · $mm^{1/2}$. Another important aspect is the contribution from the thermal residual stresses. Comparing the singularities in Figs. 7 and 8, it is obvious that this repair scheme would have appeared to be more efficient if the temperature effects had been neglected. Actually, the stress intensity factor without temperature contribution would have been 499 MPa · $mm^{1/2}$; thus the thermal residual effects lead to a 25% reduction of the effectiveness of the patch.

IV. Thermal Validation

The only results found in the literature that can be used to validate the present code are from an experiment performed by Baker et al.[2] and from an analytical study presented by Rose.[6] The former is used in this section as a test to evaluate the accuracy of the thermal residual stresses, and the latter is used to verify the effects of the surrounding structure.

A. Thermal Residual Stresses

The motivation behind the experiment of Baker et al.[2] was to develop a simple equation capable of determining postcure residual thermal stresses. Residual thermal stresses were measured on a 115 × 25 mm aluminum plate reinforced with carbon-fiber composite patches adhesively bonded to both surfaces. The physical configuration is shown in Fig. 1, and the material properties are presented in Tables 2 and 3. The properties marked with an asterisk are the ones provided in the paper.

The authors do not provide the thermal or mechanical boundary conditions or the cure or ambient temperatures. Thus, it was assumed for the present validation test that the temperature was uniform throughout the system at each time step from a cure temperature of 126°C to an ambient temperature of 21°C. Also, the

symmetry of the arrangement is exploited by modeling only one-quarter of the top half.

A first analysis was performed using a single time step for the total cooling process. For this linear analysis, the shear modulus G_a was taken to be equal to 0.5 MPa. This value was considered by the authors to be a good average value for their analytical solution to fit the experimental data.

A second calculation was completed using a nonlinear analysis. Here the temperature was uniformly decreased using 10 time steps, and G_a was updated at each time step by extrapolating the values tabulated in Table 3.

The results from the experiment and the two validation tests are presented in Fig. 9. It is shown that the results from the present code are in very good agreement with the experimental values despite the incompleteness of the data. Furthermore, it appears that the nonlinear analysis is more representative of the experimental results than the linear analysis.

Table 2 Material properties for thermal validation

Component	Property
Aluminum plate	$E_p^* = 72$ GPa
	$\nu_p = 0.3$
	$t_p^* = 1.56$ mm
	$\alpha_p^* = 23\text{E}{-6}\ ^\circ\text{C}^{-1}$
Carbon composite patch	$E_{r1}^* = 130$ GPa
	$t_r^* = 0.49$ mm
	$E_{2r} = 12$ GPa
	$\alpha_{1r}^* = 0.5\text{E}{-6}\ ^\circ\text{C}^{-1}$
	$G_r^* = 7$ GPa
	$\alpha_{2r} = 28\text{E}{-6}\ ^\circ\text{C}^{-1}$
	$\nu_{12r} = 0.3$
Adhesive layer	$G_a^* =$ Table 3
	$\nu_a = 0.3$
	$t_a^* = 0.15$ mm
	$\alpha_a = 23\text{E}{-6}\ ^\circ\text{C}^{-1}$

Table 3 Adhesive shear modulus vs temperature

G_a, GPa	Temperature, °C
0.7	20
0.8	−10
1.0	−50
1.3	−100

B. Influence of Restraint by the Surrounding Structure

Two factors that have not been mentioned so far are strongly related to the thermal residual stresses: the constraint at the edges of the plate and the extent of the plate outside the heated region. A mechanical restriction, such as clamping the edges of the plate, reduces significantly the displacement field. Similarly, if the plate is heated locally, the surrounding cool region would restrict the displacement of the heated region, inducing compressive stresses. This new displacement field in the plate can be related to an effective expansion coefficient α_p' that would produce a similar displacement field for a uniformly heated and mechanically nonrestricted structure.

Simple analytical studies of rectangular and circular plates[4,6] were performed to develop simple equations that can evaluate the effective expansion coefficient α_p' of a clamped plate subjected to a localized heating. The edges of the plate are maintained at ambient temperature in both studies.

Rose[6] considered a simple one-dimensional mathematical model of the patched region. The resulting effective coefficient of expansion is given by

$$\alpha_p' = (\alpha_p/2)(1 - L_h/L_p) \tag{3}$$

where L_h and L_p are the length of the heated region and the length of the plate, respectively.

A simple situation that corresponds to Rose's assumptions was modeled to compare the effective coefficient of expansion given by the present code. The model is illustrated in Fig. 10, and the plate is made of aluminum with the same properties as described in Table 2 except for the coefficient of thermal expansion in the x direction, which is taken to be equal to zero in order to eliminate any two-dimensional behavior.

Heating the plate to 100°C produces a state of constant thermal strain $\epsilon_y \approx 0.000805$ over the heated area. Dividing by $\Delta T = 100$°C, an effective coefficient of expansion of $\alpha_p' = 8.05\text{E}{-6}^\circ\text{C}^{-1}$ is obtained. This value is exactly the same as the one given by Eq. (3).

Although very simple, this test shows that the temperature distribution in the system as well as the relation between the displacement field and the temperature field are modeled correctly.

V. Thermal Design Study

Baker and Jones[1] suggested three approaches that could be employed to minimize residual stresses arising from patch bonding at elevated temperature.

1) The area heated should be minimized to maximize the constraint offered by the surrounding structure.

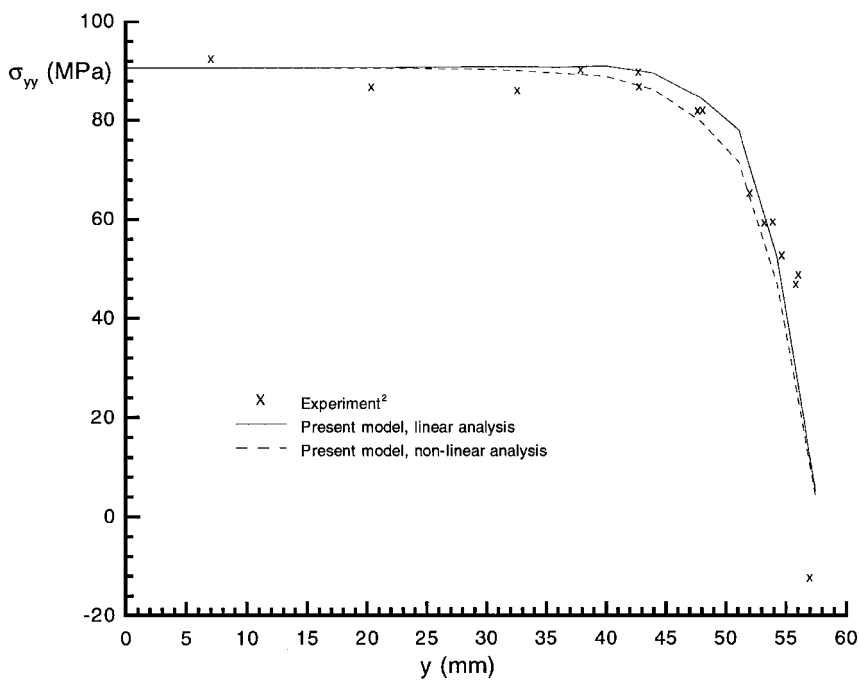

Fig. 9 Postcure residual thermal stresses for a fully symmetrically patched plate.

2) The adhesive (and if cocuring is employed, the patch) should be cured at the lowest possible temperature or precured at the lowest reasonable temperature and then postcured at a higher temperature.

3) If feasible, the patched structure should be prestressed in compression during patch application to a level that will partially or completely nullify the residual tensile stress on cooling.

No study has been found in the literature concerning these or any other recommendations.

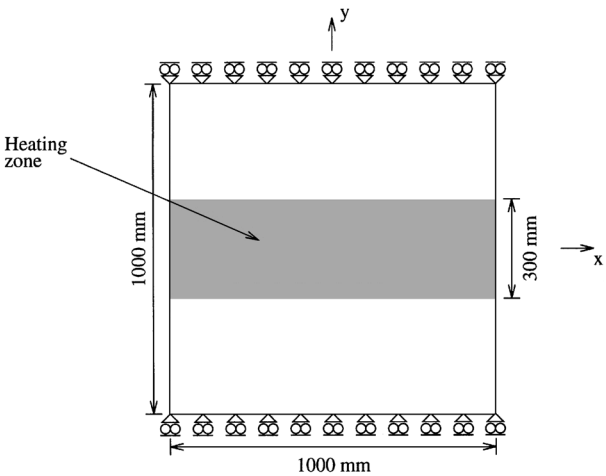

Fig. 10 Simple one-dimensional model.

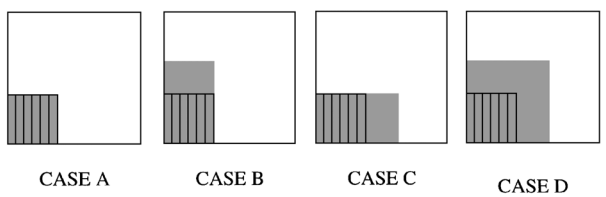

Fig. 11 Configurations used for the patch-heating-zone size and aspect-ratio study.

A. Cure Temperature and Heating Zone

The objective of this study is to evaluate the first two suggestions made by Baker and Jones.[1] This is achieved by comparing the residual tensile stress state in the plate after cooling, which indicates the severity of the residual tensile stress field under the patch. To compare the effects of the mechanical restrictions, analyses are made for unconstrained and clamped plates.

The first part of this study consists of evaluating the effects of changing the heating size and aspect ratio. Figure 11 illustrates the various configurations of the quarter-plate, where the shaded areas correspond to the heating zone, and Table 4 gives the corresponding residual thermal stress intensity factors for the free and the clamped cases. The adhesive cure temperature was chosen to be 100°C above ambient temperature.

Taking case A as a reference, it can be seen that the heating size should be minimized in the direction parallel to the crack to have a minimal state of stress around the crack when the plate is unconstrained. This is because the displacement field around the crack, and consequently the crack opening, is higher when heat is applied along the crack. However, the heating size should be maximized in the other direction to minimize the stress intensity factor when the plate is clamped. In that case, the restriction at the top edge of the plate produces a strong compressive field, closing the crack when heat is applied.

For the second part of the study, the effect of the curing temperature is illustrated in Fig. 12. It can be seen that the residual thermal stress intensity factor arising from the bonding procedure is linearly dependent on the adhesive cure temperature.

B. Thermal Effects of Fiber Orientation

This test is performed to evaluate the effects of the patch fiber orientation on the resulting postcure intensity factor. Double repairs

Table 4 Effect of heating-zone size

	K_I, MPa · mm$^{1/2}$	
Case	Free plate	Clamped plate
A	61.64	36.87
B	60.79	16.31
C	75.97	42.13
D	75.19	14.57

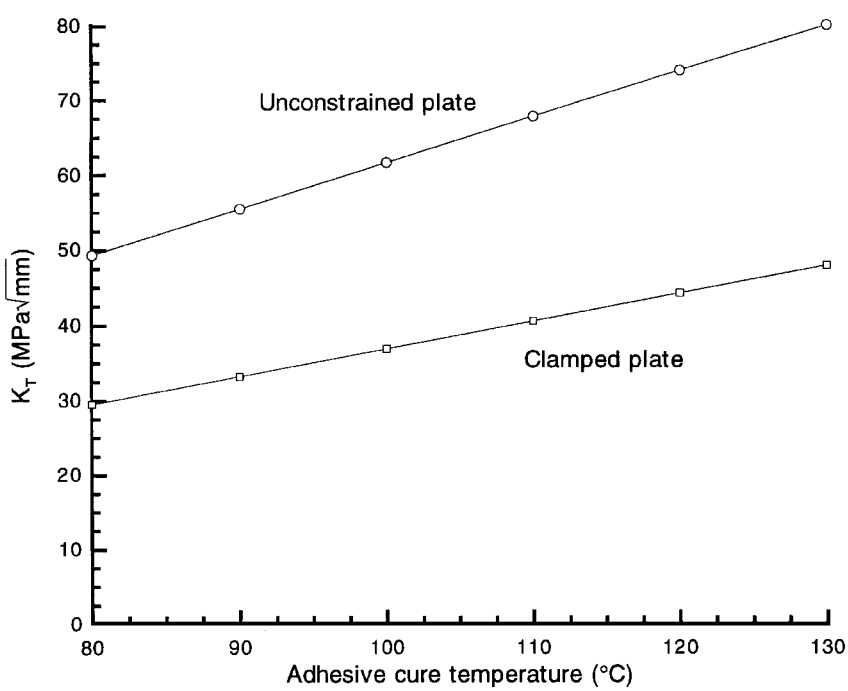

Fig. 12 Postcure thermal residual stress intensity factor for several adhesive curing temperatures.

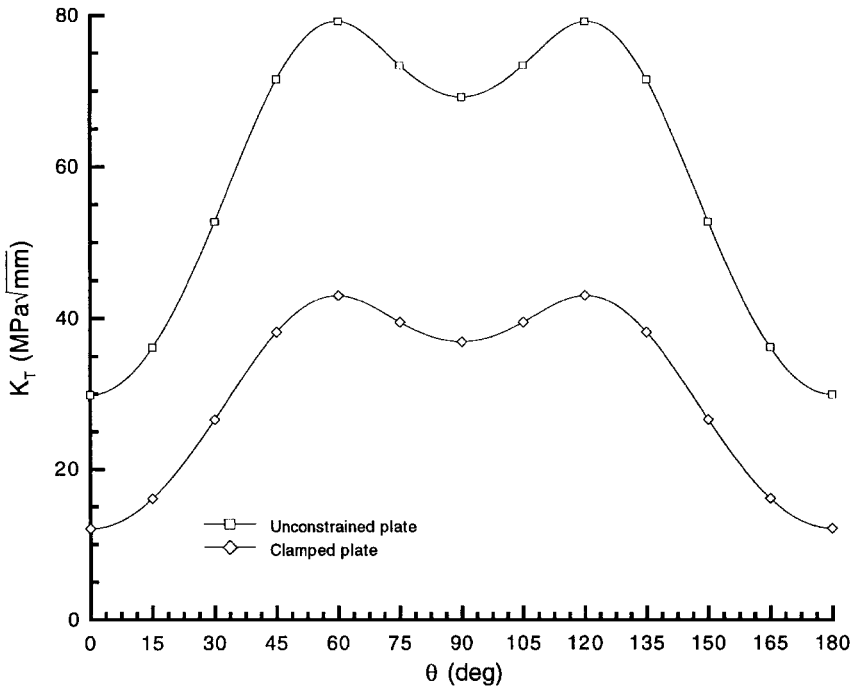

Fig. 13 Thermal stress intensity factor with respect to θ for a $[\pm\theta]_s$ patch.

made of balanced symmetric patches are analyzed for both the unconstrained and the clamped cases. The resulting stress intensity factors are plotted vs the ply angle θ for a $[\pm\theta]_s$ patch in Fig. 13, $\theta = 0$ being parallel to the crack.

It can be seen that the maximum stress intensity factor does not occur when the ply fibers are perpendicular to the crack but when the fibers are oriented at an angle of about 60 or 120 deg. These angles correspond to minima in terms of the thermal coefficient of expansion in the y direction, α_y.

VI. Summary and Conclusions

A thermal analysis code for evaluating the thermal aspects of adhesively bonded composite patches has been presented. Contrary to previous studies that considered thermal effects, the proposed model determines the actual transient temperature distribution throughout the system to evaluate the thermal stresses accurately.

It is shown that neglecting the thermal effects can lead to an overestimation of the repair efficiencies; hence, neglecting thermal effects could lead to unsafe patch designs. The thermal model of the present work provides an accurate estimation of the postcure thermal residual stresses that arise in the system. These stresses cannot be ignored and could be minimized with an adequate design with respect to several parameters such as heating-zone size and shape, cure temperature, and fiber orientation. However, one must be certain that the chosen configuration satisfies the mechanical problem, which is the reason for the existence of the patch.

References

[1]Baker, A. A., and Jones, R., *Bonded Repair of Aircraft Structure*, Martinus–Nijhoff, Dordrecht, The Netherlands, 1988, pp. 122–131.

[2]Baker, A. A., Hawkes, G. A., and Lumley, E. J., "Fibre-Composite Reinforcement of Cracked Aircraft Structures—Thermal-Stress and Thermal-Fatigue Studies," *ICCM/2: Proceedings of the 1978 International Conference on Composite Materials* (Toronto, ON, Canada), Metallurgical Society of American Inst. of Mining, Metallurgical, and Petroleum Engineers, 1978, pp. 649–668.

[3]Baker, A. A., and Jones, R., *Bonded Repair of Aircraft Structure*, Martinus–Nijhoff, Dordrecht, The Netherlands, 1988, pp. 90–92.

[4]Jones, R., and Callinan, R. J., "Thermal Considerations in the Patching of Metal Sheets with Composite Overlays," *Journal of Structural Mechanics*, Vol. 8, No. 2, 1980, pp. 143–149.

[5]Renaud, G., and Hansen, J. S., "A Quasi-Three-Dimensional Model for Cracked Structures Repaired with Composite Patches," *Canadian Aeronautics and Space Journal* (to be published).

[6]Rose, L. R. F., "A Cracked Plate Repaired by Bonded Reinforcements," *International Journal of Fracture*, Vol. 18, No. 2, 1982, pp. 135–144.

A. M. Waas
Associate Editor